



## Article

# Dynamic Distribution of *Mesanophrys* sp. and Tissue Enzyme Activities in Experimentally Infected Mud Crab *Scylla paramamosain*

Kexin Zhang<sup>1</sup>, Weiren Zhang<sup>1,2,3</sup>, Ronghua Li<sup>1,2,3,4,\*</sup>, Junkai Lu<sup>1</sup>, Qingwei Chen<sup>1</sup>, Haojie Hu<sup>1</sup>, Fei Yin<sup>1,2,3,4</sup>, Changkao Mu<sup>1,2,3,4</sup>, Weiwei Song<sup>1,2,3,4</sup> and Chunlin Wang<sup>1,2,3,4</sup>

<sup>1</sup> Key Laboratory of Aquacultural Biotechnology, Ningbo University, Chinese Ministry of Education, Ningbo 315211, China

<sup>2</sup> Collaborative Innovation Center for Zhejiang Marine High-Efficiency and Healthy Aquaculture, Ningbo 315211, China

<sup>3</sup> Marine Economic Research Center, Donghai Academy, Ningbo University, Ningbo 315211, China

<sup>4</sup> Key Laboratory of Green Mariculture (Co-Construction by Ministry and Province), Ministry of Agriculture and Rural, Ningbo 315211, China

\* Correspondence: lironghua@nbu.edu.cn

**Abstract:** *Mesanophrys* sp. is reported to be highly pathogenic to marine crustaceans. This study presents the first report of *Mesanophrys* sp. infection in the mud crab (*Scylla paramamosain*). In this study, we first recorded the survival rates of an experimentally infected group and a control group; the cumulative survival rate in the infected group was significantly lower compared to the control group after 72 h (73.20% vs. 94.19%), while the highest mortality of *S. paramamosain* occurred within the first 24 h post-infection. Then, we investigated the dynamic distribution and tissue tropism of the *Mesanophrys* sp. in the infected *S. paramamosain* by a quantitative real-time polymerase chain reaction (qPCR). The result showed that a significant increase in the number of *Mesanophrys* sp. could be detected in all tested tissues (obtained from the eyestalks, gills, heart, nerves, muscles and hepatopancreas) at 3 h post-infection. The numbers of *Mesanophrys* sp. in the gill, eyestalk and nerve tissues were relatively higher than in the other tissues. The gill tissue showed the highest numbers from 6 to 48 h. Histopathological observation found a severe collapse in the filament structure, which indicated tissue-specific pathogen infection. Furthermore, the antioxidant enzyme activity of superoxide dismutase (SOD), catalase (CAT) and peroxidase (POD) in three representative tissues (gill, muscle and hepatopancreas) were compared between the infected and control groups, and a significant increase in enzyme activity was observed in all three tested tissues in the infected group, indicating a relatively strong innate immune defense reaction that could have been induced by *Mesanophrys* sp. infection. These results will be helpful to *Mesanophrys* sp. pathogenicity-related research and the control of this pathogen in *S. Paramamosain* in the future.

**Keywords:** *Scylla paramamosain*; *Mesanophrys* sp.; tissue distribution; qRT-PCR; antioxidant enzyme activity

**Key Contribution:** (1) Most *S. paramamosain* mortality (22.88%) occurs within 24 h post *Mesanophrys* sp. infection. (2) A significant increase in the number of *Mesanophrys* sp. could be detected in all tested tissues, and the gill was the main target of *Mesanophrys* sp. (3) The activity of antioxidant enzymes was significantly increased in the infected group, indicating that the immune defenses of *S. paramamosain* had been triggered by *Mesanophrys* sp. infection. *Mesanophrys* sp. infection significantly increased POD, CAT and SOD activity in the three tissues.



**Citation:** Zhang, K.; Zhang, W.; Li, R.; Lu, J.; Chen, Q.; Hu, H.; Yin, F.; Mu, C.; Song, W.; Wang, C. Dynamic Distribution of *Mesanophrys* sp. and Tissue Enzyme Activities in Experimentally Infected Mud Crab *Scylla paramamosain*. *Fishes* **2023**, *8*, 249. <https://doi.org/10.3390/fishes8050249>

Academic Editors: Yongxu Cheng, Chaoshu Zeng, Fang Wang, Boping Tang and Yunfei Sun

Received: 9 February 2023

Revised: 18 April 2023

Accepted: 20 April 2023

Published: 8 May 2023



**Copyright:** © 2023 by the authors. Licensee MDPI, Basel, Switzerland. This article is an open access article distributed under the terms and conditions of the Creative Commons Attribution (CC BY) license (<https://creativecommons.org/licenses/by/4.0/>).

## 1. Introduction

Mud crabs of the genus *Scylla* are an economically important crustacean species, with high demand in southeast Asian countries [1,2]. Currently, there are four known species in the genus *Scylla*: *S. olivacea*, *S. paramamosain*, *S. serrata* and *S. tranquebarica*, all of which have been commercially farmed [3,4]. Historically, *S. paramamosain* has been one of the most economically important marine crustaceans along the coastal provinces of southern China. However, with the rapid expansion of the mariculture industry, the outbreak of disease caused by pathogens has become more and more frequent, causing significant economic loss. A rising number of reports have shown that the *S. paramamosain* aquaculture industry is threatened by diseases caused by pathogens (such as white spot syndrome virus disease [WSSV], *Vibrio alginolyticus*) [5,6].

*Mesanophrys* ciliates belong to the *Orchitophryidae* family, which is widely distributed in marine environments. Most *Mesanophrys* ciliates feed on bacteria and organic debris [7] and grow quickly through a two-division proliferation mode. However, they can also invade the hemolymphs of crustaceans and consume the lysate therein in order to proliferate; intense infection causes damage to the internal organs and finally leads to death, which may cause serious economic losses to local farmers and enterprises [8–11]. In early 2017, a new parasite, *Mesanophrys* sp., emerged in an artificial nursery farm of *Portunus trituberculatus* in Ningbo, Zhejiang Province, resulting in more than 80% mortality among the *P. trituberculatus* [12]. *S. paramamosain* is another of the major aquaculture crabs in Zhejiang Province; some *P. trituberculatus* pathogens such as *Hematodinium* sp. and *Aquimarina hainanensis* have been proven to be harmful to mud crabs. [13–15]. However, the infection effects and distribution dynamics of *Mesanophrys* sp. on *S. paramamosain* have not yet been evaluated.

The qPCR is one of the most effective methods for the sensitive detection of pathogens and has been widely used for pathogen diagnosis, including of viruses, bacteria, oomycetes and fungi from a wide variety of hosts [16,17]. In this study, we established a qPCR-based method to determine the dynamic distribution of *Mesanophrys* sp. in experimentally infected *S. paramamosain*; the activities of three antioxidant enzymes (POD, CAT and SOD) were also investigated in representative tissues (gill, muscle and hepatopancreas). These results could provide a theoretical basis for understanding the dynamic distribution of *Mesanophrys* sp. in *S. paramamosain* tissues and the relationship between this parasite and the antioxidant system.

## 2. Materials and Methods

### 2.1. Experimental Animals and Conditions

Three hundred and thirty *S. paramamosain* (body weight of  $50 \pm 5$  g) were obtained from a farm pond in Fenghua City, Zhejiang Province, China. During the entire experiment, crabs were fed with fresh clams once a day at 7:00 p.m. (around 3% of the crabs' body weight), and one third of the water was changed daily with the removal of uneaten feed. During the experiment, aeration and water exchange were applied to control water quality. The main physicochemical indicators of water quality were measured using a water quality meter (Horiba U54G; Horiba Instruments Limited, Kyoto, Japan) and maintained as follows: water temperature 22–25 °C, salinity 25 psu, pH  $8.25 \pm 0.25$ , water-dissolved O<sub>2</sub> > 6.0 mg/L, ammonia nitrogen (NH<sub>3</sub>-N) < 0.05 mg/L.

Prior to the experiment, 20 crabs were randomly selected for *Mesanophrys* sp. detection using the qPCR method (see below); no evidence of infection was found.

### 2.2. *Mesanophrys* sp. Cultivation

The *Mesanophrys* sp. was provided by the Laboratory of Aquatic Animal Disease, Ningbo University, and was cultivated following Cain's method [18]. Simply, the *Mesanophrys* sp. was cultivated in a sterile 25 cm<sup>2</sup> tissue-culture flask (BD) 50 mL culture medium. The culture medium contained sterilized sea water (salinity = 25 psu), 10% (v/v) heat-inactivated fetal bovine serum (FBS, Gibco, Billings, MT, USA) and 5% crab soup (100 g crab muscle and 1000 mL water, boiled to 100 mL). The temperature was maintained at 12–14 °C. In order to

observe its growth curve, the number of ciliates contained in 10  $\mu$ L of the culture medium was counted three times at 0, 6, 12, 18, 24, 30, 36, 42, 48, 54, 60, 66, 72, 78, 84 and 90 h using light microscopy (Nikon Eclipse Ni-U) as described by Parama [19].

### 2.3. Infection of Experimental Animals

Three hundred crabs were randomly selected from the total three hundred and ten crabs and allocated into infected and control groups with three replicates in each group. *Mesanothryx* sp. infection was performed using the method described by Stentiford and Shields [20]. Simply, 70% ethanol was used to sterilize the surface of the crab. Then, *Mesanothryx* sp. (10  $\mu$ L/g, diluted from 48 h cultivation) suspended in sterilized saline solution was injected into the infected group at the juncture of the fifth walking leg, while sterilized saline solution was injected into the control group.

The survival rate of the mud crabs was recorded at an interval of 12 h until 72 h post-infection. Five live crabs were randomly selected for tissue collection (including muscle, gill, heart, hepatopancreas, nerve and eyestalk) at 0, 3, 6, 9, 12, 24, 36 and 48 h. All the tissues were divided into three parts; two parts were stored in liquid nitrogen for enzyme activity determination, DNA extraction and qRT-PCR detection of *Mesanothryx* sp. The other part was fixed with Bouin's solution for paraffin slices.

Tissues were first detected by qPCR to investigate the dynamic distribution of *Mesanothryx* sp. in the experimentally infected crabs; then, representative tissues were selected for antioxidant enzyme activity measurement and histology observation.

### 2.4. Detection and Quantification of *Mesanothryx* sp. in Tissues

Serial 10-fold dilutions containing copies of  $10\text{--}10^5$  cells/mL were used as templates to prepare the standard curve. DNA was extracted using DNA Kit (Axygen A Corning Brand, Suzhou, China); the target gene of *Mesanothryx* sp. was amplified using forward primer (ITS1-5.8s-ITS2F and ITS1-5.8s-ITS2R) [11] (Table 1). Quantitative real-time PCR assays were carried out in triplicate in a 20  $\mu$ L final volume that included 1  $\mu$ L of DNA template, 10  $\mu$ L 2  $\times$  of MagicSYBR Mixture (CWBIO, Beijing, China), 0.4  $\mu$ L of each primer (10  $\mu$ M) and 8.2  $\mu$ L of nuclease-free water. The qPCR reaction was conducted in an 8-tube strip using an LightCycler480 instrument (Roche, Switzerland) under the following conditions: 94  $^{\circ}$ C for 10 min, 40 cycles of denaturation for 30 s at 94  $^{\circ}$ C, annealing for 30 s at 65  $^{\circ}$ C and elongation for 10 min at 72  $^{\circ}$ C. The dilutions were tested in triplicate and used as quantification standards to construct the standard curve by plotting the copy number logarithm against the cycle threshold (Ct) values.

**Table 1.** Primers used in this study.

Primer	Sequence (5'–3')	PCR Objective
ITS1-5.8s-ITS2F	GTAGGTGAACCTGCGGAAGGATCATTA	qPCR
ITS1-5.8s-ITS2R	TACTGATATGCTTAAGTTCAGCGG	qPCR

Total DNA was extracted from the muscle, gill, heart, hepatopancreas, nerve and eyestalk tissue of crabs. Generally, 0.1 g of each tissue specimen was weighed and added into 500  $\mu$ L of phosphate buffered saline, and the sample was homogenized and centrifugated. DNA was extracted from a 200  $\mu$ L supernatant of the tissue homogenates using DNA Kit (Axygen A Corning Brand, Suzhou, China) and stored at  $-80^{\circ}$ C. The parasite's load was quantified by a qPCR using 2  $\mu$ L of DNA per reaction. The DNA copy number was converted to copy number per gram using the calculated Ct-value determined from the standard curve. Each sample was tested in triplicate.

### 2.5. Histology Observation

Histology was used to determine whether any host response was present. The fixed tissue samples were dehydrated using 60%, 70%, 80%, 90%, 95% and 100% graded ethanol and clarified in a 1:1 mixture of absolute ethanol and xylene for 15 min. Then, the tissue

was transparented using xylene for 15 min (this step needed to be repeated twice) and transferred into a 1:1 mixture of xylene and paraffin for 15 min, followed by transferal to liquid wax at 60 °C for 60 min (repeated twice). Later, the tissue was sliced with a table microtome (Leica RM2016, Leica Biosystems, Wetzlar, Germany) at a thickness of 5 µm; the cross sections were obtained and tiled onto glass slides then stained using hematoxylin and eosin (H.E). Finally, the slices were mounted using neutral gum and observed through light microscopy (OLYMPUS BX60, Olympus Optical Co., Tokyo, Japan), and digital images were taken using an imaging system (OLYMPUS DP72, Olympus Optical Co., Tokyo, Japan).

## 2.6. Antioxidant Enzyme Activity Analysis

The tissue was precisely weighed ( $0.1 \pm 0.05$  g) and diluted with 1 mL of physiological saline solution 0.9% (Sterile). Then, the supernatant was obtained after a 10 min centrifugation at 2500–3000 rpm (4 °C). Enzyme activity in the gill, muscle and hepatopancreas tissue was determined using commercial kits provided by Jiancheng Biotechnology Research Institute (Nanjing, China) in the following order: superoxide dismutase (SOD, A001-3-1), catalase (CAT, A007-1-1), peroxidase (POD, A084-1-1). They were measured using a UV-spectrophotometer (Beijing Purkinje General Instrument Co., Ltd. Beijing, China) at 550 nm, 405 nm and 420 nm, respectively, as described by the manufacturer's protocols.

## 2.7. Statistical Analysis

Differences in the survival rate between the infected group and the control group were analyzed by the log rank test using the GraphPad Prism 8 software. A one-way ANOVA with Tukey's multiple comparisons was conducted to compare the parasite load at different time points using the SPSS 22 software, and the Games–Howell test was performed when the assumption of homogeneity of variances was violated. The independent samples *t*-test was used to compare the activities of antioxidant enzymes between the control group and the infected group.  $p < 0.05$  was considered to be a significant difference.

# 3. Results

## 3.1. Growth Curve of *Mesanoophrys* sp. and Establishment of the Standard Curve for qPCR Detection

The results revealed that the number of *Mesanoophrys* sp. rose rapidly from 24 h and reached its peak at 48 h. The number of ciliates remained above 60 cells/µL from 60 h to 72 h. (Figure 1A). At 48 h, ciliates were collected and diluted for the establishment of the standard curve for qPCR detection and injection into the infected group.

The qPCR amplification curves were generated using 10-fold dilutions of *Mesanoophrys* sp. with specific primers (Figure 1B). A strong linear relationship was shown between Ct values and the log copy number of the standard controls (Figure 1C, D), with a correlation coefficient of  $R^2 = 0.9918$ ; the following formula:  $Y = -3.3327X + 31.773$  was achieved ( $Y$  = threshold cycle,  $X$  = natural log of concentration (cells/mL), and concentration above 10 ind/mL was theoretically considered detectable.

## 3.2. Survival Curve of Crabs in Infected and Control Group

The average survival rate of mud crabs in the infected and control groups over 72 h are presented in Figure 2. The cumulative survival rate in the infected group was significantly lower compared to the control group after 72 h (73.20% vs. 94.19%,  $p < 0.05$ , log-rank test, degree of freedom ( $df = 1$ ),  $p = 0.0005$ ). Notably, the cumulative survival rate in the infected group decreased to 77.12% in the first 24 h post-infection, indicating that the highest mortality was found during 24 h. Comparison of survival rates at each time point demonstrated that the survival rate in the infected group reached a bottom at 24 h point (Figure 2B).

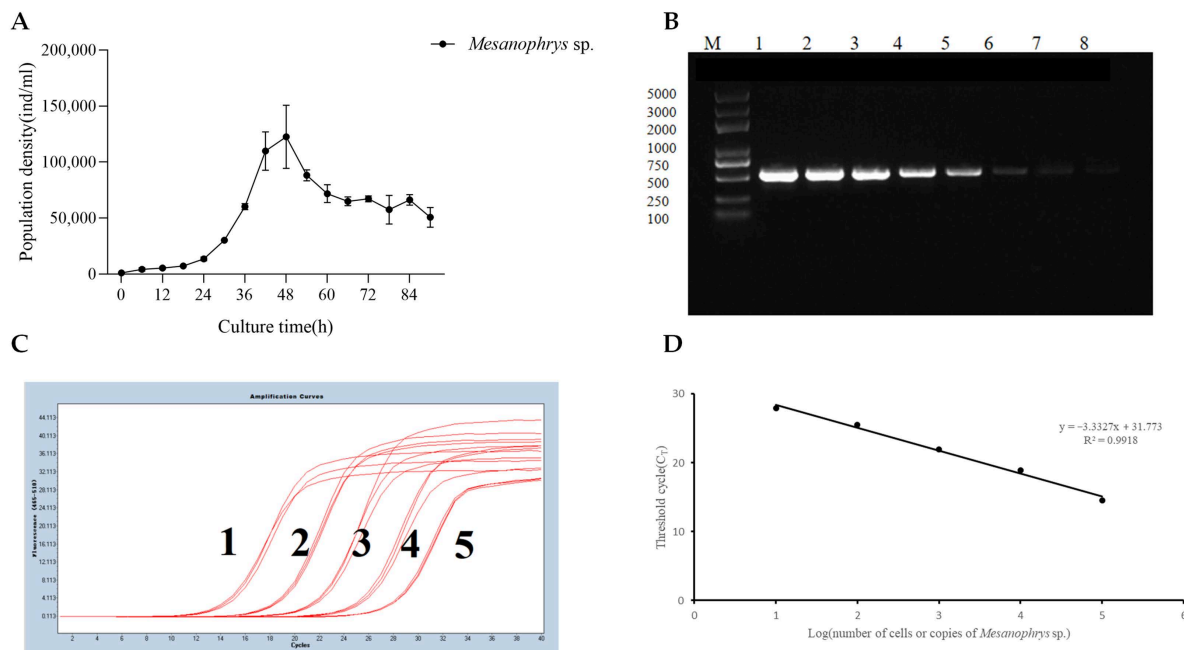


**Figure 1.** Culture and detection of *Mesanophrys* sp. based on the qPCR method. (A) Growth curve of *Mesanophrys* sp.; (B) Specificity and sensitivity quantitative detection of *Mesanophrys* sp. (Line 1, 2, 3, 4, 5, 6, 7, 8 representing *Mesanophrys* sp. of  $10^8$ ,  $10^7$ ,  $10^6$ ,  $10^5$ ,  $10^4$ ,  $10^3$ ,  $10^2$ ,  $10$  ind/mL, respectively; (C) Determination of *Mesanophrys* sp. copies using a qPCR. (Line 1, 2, 3, 4, 5 represent *Mesanophrys* sp. of  $10^2$ ,  $10^3$ ,  $10^4$ ,  $10^5$  copies/mL, respectively; (D) Standard curve of the qPCR assay for the detection of *Mesanophrys* sp.

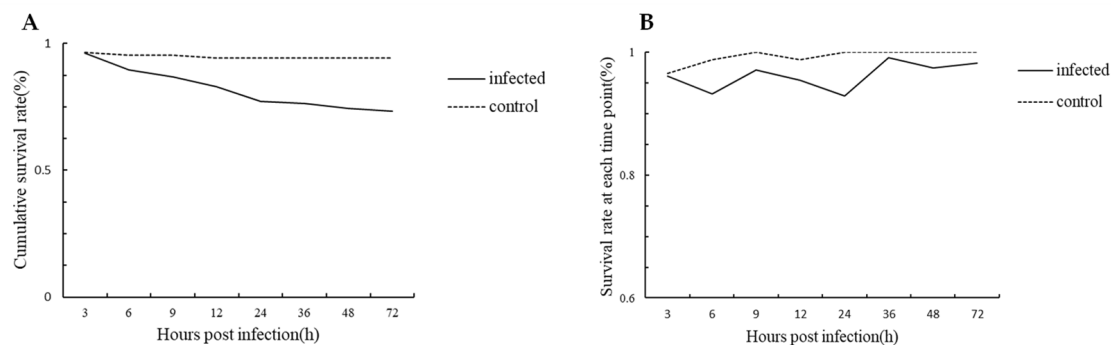


**Figure 2.** Summary of the survival rate of *S. paramamosain*. (A) Cumulative survival rate of *S. paramamosain* during 72 h; (B) Survival rate at each time point during 72 h.

### 3.3. Tissue Distribution of *Mesanophrys* sp.

In the present study, an obvious increase in *Mesanophrys* sp. could be detected in all six tissues post-infection by the qPCR as early as 3 h. (Figure 3). In the gill, nerve and eyestalk tissues, the parasitic copy number was higher than that in the heart, muscle and hepatopancreas tissues. The highest load of *Mesanophrys* sp. in the six tissues according to the log copy number (from high to low) were as follows: gill ( $5.85 \times 10^3$  copies/g), eyestalk ( $4.56 \times 10^3$  copies/g), nerve ( $3.22 \times 10^3$  copies/g), heart ( $1.21 \times 10^3$  copies/g), muscle ( $3.85 \times 10^2$  copies/g) and hepatopancreas ( $2.06 \times 10^2$  copies/g). After infection, the parasitic DNA loads in the heart, hepatopancreas, gill, nerve, muscle and eyestalk tissues increased to a peak point at 3 h, 3 h, 6 h, 9 h, 9 h and 24 h, respectively, then decreased in the heart, nerve, muscle and eyestalk tissues but fluctuated in the gill and hepatopancreas tissues. The number of parasites was significantly different between time points in the heart ( $F_A = 41.971$ ,  $df_1 = 7$ ,  $df_2 = 6.189$ ,  $p = 0.035$ ), nerve ( $F = 256.242$ ,  $df_1 = 7$ ,  $df_2 = 16$ ,  $p < 0.001$ ), gill ( $F_A = 92.443$ ,  $df_1 = 7$ ,  $df_2 = 6.068$ ,  $p = 0.018$ ), muscle ( $F_A = 83.806$ ,



$df_1 = 7$ ,  $df_2 = 6.578$ ,  $p = 0.030$ ), hepatopancreas ( $F = 8.341$ ,  $df_1 = 7$ ,  $df_2 = 16$ ,  $p < 0.001$ ) and eyestalk tissues ( $F_A = 54.451$ ,  $df_1 = 7$ ,  $df_2 = 6.111$ ,  $p < 0.001$ ). In particular, the parasitic load in the gill tissue maintained a relatively high level from 6 to 48 h.

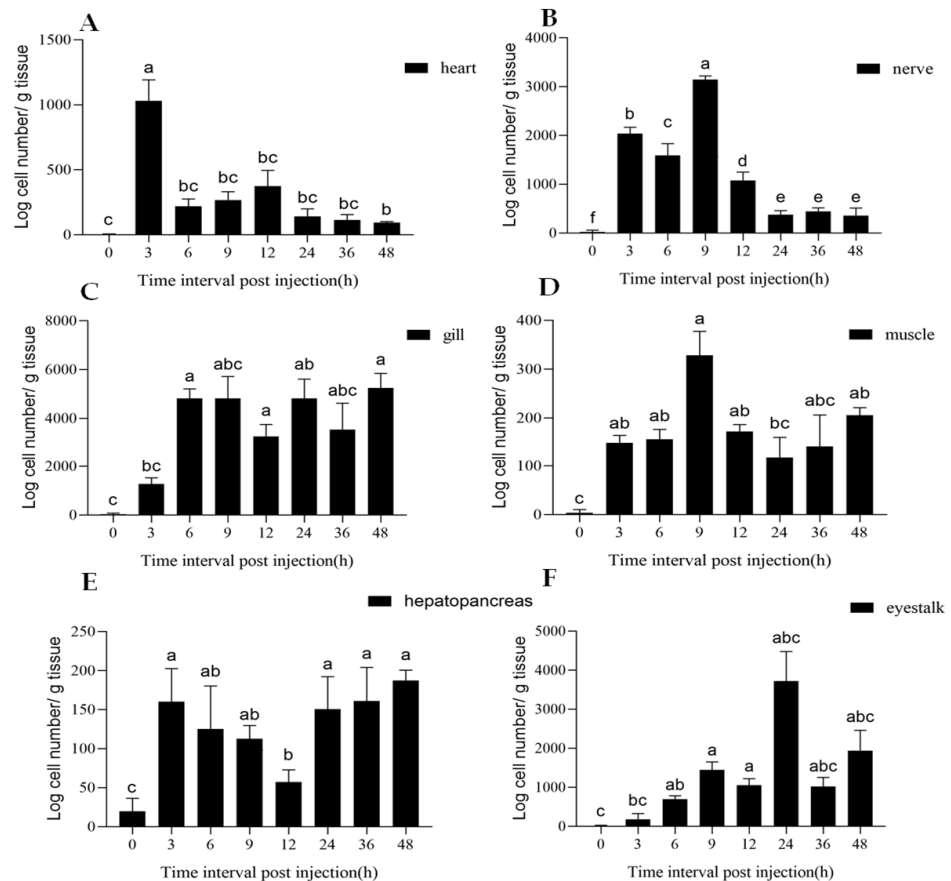


**Figure 3.** The proliferation of *Mesanophrys* sp. in the (A) heart, (B) nerve, (C) gill, (D) muscle, (E) hepatopancreas and (F) eyestalk tissues. The results are based on three biological repeats and expressed as means  $\pm$  SE. Different superscripts (i.e., a–e) represent significant differences at different time points at  $p < 0.05$  level.

### 3.4. Histopathology

Histopathological observation of the gill tissue sampled at 9 h revealed an obvious difference between the control and infected groups (Figure 4). In the gill tissue of a healthy crab from the control group, the gill filaments were arranged in order with complete structure. In the haemal channel, there was a reticular trabecular cell structure formed by specialized pilaster cells. However, in the infected group, some pilaster cells were disrupted in the gill filaments, which caused a disarrangement of the secondary lamellae. The gill tissue in the infected group showed a detached cuticle, swelling at the end of the gill filament and disruption of the pilaster cells. Moreover, obvious hemocyte nodules appeared in the gill tissue of the infected group.

### 3.5. Antioxidant Enzyme Activity

Compared to the control group, the activities of three antioxidant enzymes (POD, CAT, SOD) in three tissues (gill, muscle and hepatopancreas) were upregulated in the infected group at certain time points (Figure 5).

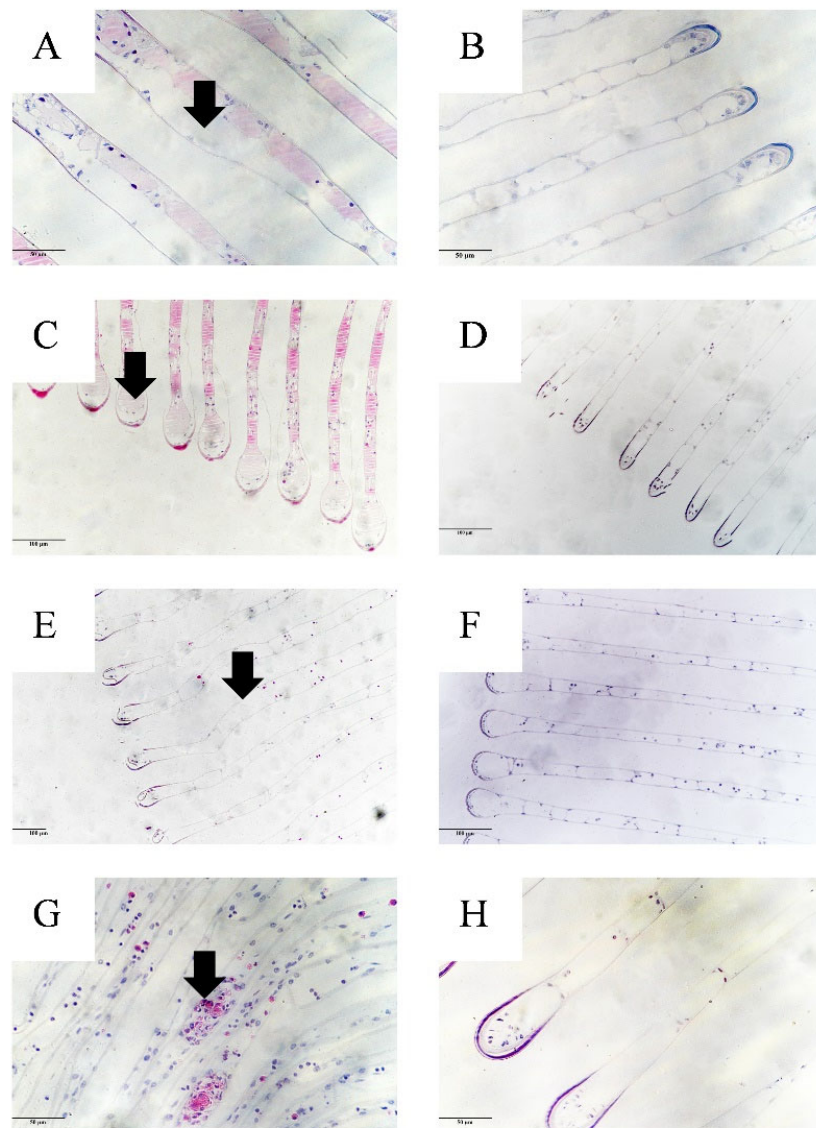


**Figure 4.** Alterations observed in a branch filament of *S. paramamosain*. (A,C,E,G) represent the infected group while (B,D,F,H) represent the control group. Arrows indicate (A) Detached cuticle; (C) Swelling of the gill filament; (E) Disruption of the pilaster cells; (G) Hemocyte nodules. Scale (A,B,G,H) = 50  $\mu\text{m}$ , (C–F) = 100  $\mu\text{m}$ .

POD activity in the hepatopancreas tissue of the infected group increased and was significantly higher than the control group from 3 to 9 h ( $df = 4$ ,  $T_{3h} = -7.536$ ,  $p_{3h} = 0.002$ ;  $T_{6h} = -5.987$ ,  $p_{6h} = 0.004$ ;  $T_{9h} = -9.143$ ,  $p_{9h} < 0.001$ ); then, it decreased and maintained a low level from 12 h. In the gill tissue, it increased and was significantly higher than the control group from 3 to 24 h ( $df = 4$ ,  $T_{3h} = 5.705$ ,  $p_{3h} = 0.005$ ;  $T_{6h} = 12.295$ ,  $p_{6h} < 0.001$ ;  $T_{9h} = 4.836$ ,  $p_{9h} = 0.008$ ;  $T_{12h} = 4.964$ ,  $p_{12h} = 0.008$ ;  $T_{24h} = 4.580$ ,  $p_{24h} = 0.010$ ); then, it decreased from 36 h. In the muscle tissue, it increased and was significantly higher than the control group from 12 to 36 h ( $df = 4$ ,  $T_{12h} = -3.806$ ,  $p_{12h} = 0.019$ ;  $T_{24h} = -5.336$ ,  $p_{24h} = 0.027$ ;  $T_{36h} = -5.243$ ,  $p_{36h} = 0.006$ ) before decreasing at 48 h.

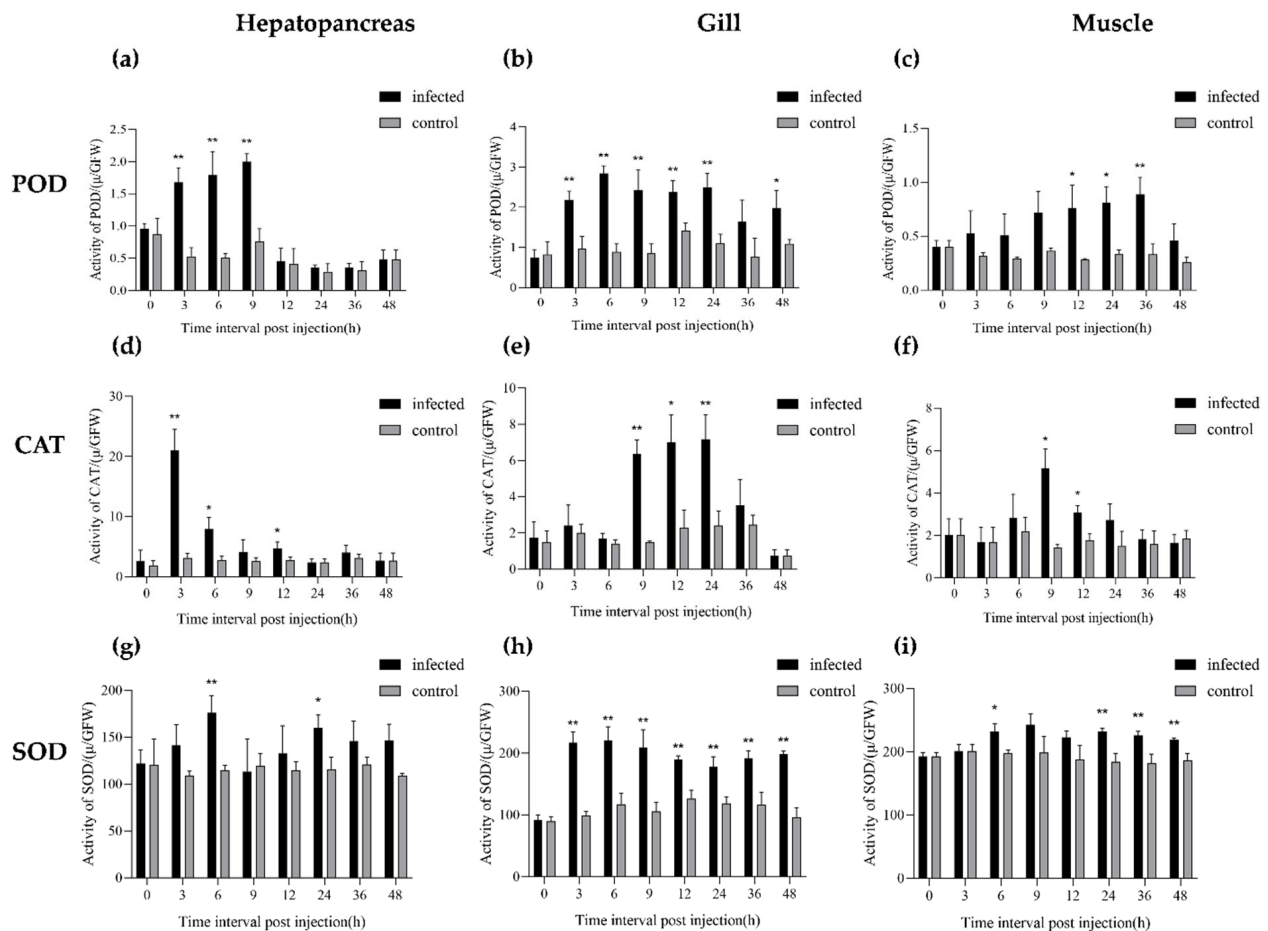


**Figure 5.** Changes in CAT, POD and SOD activity in different tissues. POD activity in the (a) hepatopancreas, (b) gill and (c) muscle tissues; CAT activity in the (d) hepatopancreas, (e) gill and (f) muscle tissues; SOD activity in the (g) hepatopancreas, (h) gill and (i) muscle tissues. The results are based on three biological repeats and expressed as means  $\pm$  SE. Statistically significant differences between the infected group and control group at the same time point are indicated by asterisks (\*  $p < 0.05$ , \*\*  $p < 0.01$ ).

CAT activity in the hepatopancreas tissue of the infected group increased and was significantly higher than the control group from 3 to 6 h ( $df = 4$ ,  $T_{3h} = -8.586$ ,  $p_{3h} = 0.010$ ;  $T_{6h} = -4.347$ ,  $p_{6h} = 0.012$ ), then decreased and maintained a low level from 9 h. In the gill tissue, CAT activity in the infected group sharply increased and was significantly higher than the control group from 9 to 24 h ( $df = 4$ ,  $T_{9h} = 11.584$ ,  $p_{9h} < 0.001$ ;  $T_{12h} = 4.498$ ,  $p_{12h} = 0.011$ ;  $T_{24h} = 5.270$ ,  $p_{24h} = 0.006$ ), then decreased from 36 h. In the muscle tissue, it peaked at 9 h and was significantly higher than that of the control group ( $df = 4$ ,  $T = -6.934$ ,  $p_{9h} = 0.018$ ), then decreased from 12 h.

SOD activity in the hepatopancreas tissue of the infected group increased and was significantly higher than the control group at 6 h ( $df = 4$ ,  $T = -6.534$ ,  $p_{6h} = 0.005$ ), then decreased from 9 h. In the gill tissue, it increased from 3 to 48 h and was significantly higher than the control group ( $df = 4$ ,  $T_{3h} = -10.821$ ,  $p_{3h} < 0.001$ ;  $T_{6h} = -6.369$ ,  $p_{6h} = 0.003$ ;  $T_{9h} = -5.543$ ,  $p_{9h} = 0.005$ ;  $T_{12h} = -7.386$ ,  $p_{12h} = 0.002$ ;  $T_{24h} = -5.356$ ,  $p_{24h} = 0.006$ ;  $T_{36h} = -5.458$ ,  $p_{36h} = 0.005$ ;  $T_{48h} = -11.010$ ,  $p_{48h} < 0.001$ ). In the muscle tissue, it increased significantly from 6 h ( $df = 4$ ,  $T_{6h} = -4.198$ ,  $p_{6h} = 0.014$ ) and maintained a higher level than the control group at 24, 36 and 48 h ( $df = 4$ ,  $T_{6h} = -4.198$ ,  $p_{6h} = 0.014$ ;  $T_{24h} = -5.671$ ,  $p_{24h} = 0.005$ ;  $T_{36h} = -4.700$ ,  $p_{36h} = 0.009$ ;  $T_{48h} = -4.993$ ,  $p_{48h} = 0.008$ ).



#### 4. Discussion

*Mesanophrys* sp. is one of the newest confirmed ciliated parasites infecting marine crabs and was responsible for the “parasitosis” outbreak in *P. trituberculatus* [21]. Our study appears to be the first to report the dynamic distribution of *Mesanophrys* sp. and tissue enzyme activities in the mud crab (*S. paramamosain*) and provides basic biological information for the prevention and control of *Mesanophrys* sp. infection in *S. paramamosain*.

According to the survival curve of *S. paramamosain*, the highest mortality of the infected group occurred during the first 24 h post-infection, and the total mortality rate was 26.80% over 72 h, which was lower than that of *P. trituberculatus* (mortality rate over 80%) [11], indicating a species-specific pathogen infection characteristic in *Mesanophrys* sp., which would also suggest that the first 24 h post-infection should be the key period to for controlling the disease in *S. paramamosain*.

A qPCR provides a sensitive, easy-to-perform and rapid method for pathogen quantification in crustaceans [22,23]. In this study, we established a qPCR assay for the detection and quantification of *Mesanophrys* sp. in experimentally infected samples based on a primer set targeting the ITS1-5.8s-ITS2 region of the rRNA gene; the correlation coefficient of  $R^2$  was close to 1, indicating that this method is highly efficient, which provides a suitable approach for *Mesanophrys* sp. diagnosis.

In the present study, the loads of *Mesanophrys* sp. were found by the qPCR to be widely distributed in various tissues in the artificial infection samples as early as 3 h; the rapid spread of parasites may have been through the circulatory system. In the gill, nerve and eyestalk tissues, the parasitic copy number was higher than that in the heart, muscle and hepatopancreas tissue, demonstrating a tissue-specific pathogen tropism. It is particularly worth noting that the parasitic loads in the gill tissue maintained a relatively high level from 6 to 48 h and exhibited the highest parasitic loads ( $5.85 \times 10^3$  copies/g) among all the tissues. Histopathological observation also found that the accumulation of a large number of *Mesanophrys* sp. caused obvious damage to the gill tissue, as shown by the detached cuticle, the swelling gill filament and hemocyte nodules. The expansion and deformation of the gill lamella caused by *Mesanophrys* sp. in *P. trituberculatus* was also reported by Liu et al. [11]. Based on these results, the gill tissue could be considered the main target of *Mesanophrys* sp. and the first choice of tissue for detecting *Mesanophrys* sp. in infected *S. paramamosain*.

Histopathology revealed that the gill filament of the infected *S. paramamosain* appeared slightly swollen, accompanied by a detached cuticle. These alterations in the gill surface architecture can reduce the gaseous exchange capacity of the gills [24]. It has been reported that some ciliates such as *Synophrya* sp. could infect the gills of its crustacean host and cause mortality at certain life-cycle stages, which is generally attributed to poor gas exchange across the gills [25,26]. In this study, the damage to the gill tissue caused by the accumulation of a large number of *Mesanophrys* sp. could also have been the main cause of the deaths of the *S. paramamosain*. Furthermore, relatively higher pathogen loads were detected in the nerve and eyestalk tissue, which may be conducive to *Mesanophrys* sp. pathogenicity-related research in the future.

Reactions which occur when a host is subjected to biotic or abiotic stresses often result in the production of reactive oxygen species (ROS) [including superoxide ion ( $O_2^{\cdot-}$ ), hydroxyl radical ( $\cdot OH$ ) and hydrogen peroxide ( $H_2O_2$ )]; these cellular oxidants play an important role in antimicrobial cell defense, protecting the host against a large number of pathogenic microorganisms [27,28]. However, the excessive accumulation of ROS could cause serious oxidative damage to cell components including lipids, membranes, proteins and DNA, resulting in various diseases [29]. To ameliorate the danger posed by the presence of cellular oxidants, complex defense mechanisms have evolved, including the synthesis of antioxidants such as ascorbate and glutathione and an increase in the activity of antioxidant enzymes which play an important role as ROS-detoxifying proteins [e.g., superoxide dismutase (SOD), ascorbate peroxidase (APX), catalase (CAT), glutathione peroxidase (GPX) and peroxidase (POD)] [30–32].

In this study, according to the results of the tissue distribution of *Mesanoophrys* sp., we selected gill tissue with relatively higher pathogenic accumulation and muscle tissue with lower pathogenic accumulation to investigate changes in antioxidant enzyme activity. Additionally, in crustaceans, the hepatopancreas (considered to be homologous to the mammalian liver and pancreas), which was also included in the analysis of antioxidant enzyme activity, plays a crucial role in the metabolism system and innate immunity [33]. The results indicated that *Mesanoophrys* sp. infection significantly increased POD, CAT and SOD activity in the three tissues ( $p < 0.05$ ). In the antioxidant system, SOD and CAT work together protecting the cells from hydrogen peroxide poisoning: SOD catalyzes the dismutation of superoxide anions to hydrogen peroxide, which is subsequently detoxified to oxygen and water by CAT or GPX [34]. In our study, SOD and CAT showed significant upregulation in the three tissues compared to the control group, suggesting that they may clear superoxide free radicals and enhance the antioxidant capacity of cells instead of directly acting on the pathogen at the tissues. The significant up-regulation of SOD and CAT in the gill tissue lasted longer than that in the hepatopancreas and muscle tissue, which may be due to a large number of pathogens accumulated in the gill tissue, inducing a relatively strong innate immune defense reaction. The enzyme activity of CAT in the hepatopancreas tissue increased rapidly at 3 h post-infection and was almost 3-fold compared to the gill and muscle tissues. This may be due to the amount of CAT in the hepatopancreas being naturally higher than in other organs, which could enable it to decompose hydrogen peroxide more efficiently [35].

Peroxidases are enzymes capable of reducing hydrogen peroxide and other hydroperoxides to water, and they can be found in a wide variety of organisms [33]. In our study, POD activity in the three tissues of the infected group was significantly higher than in the control group at certain time points, indicating that defense against the pathogen was triggered in the infected crabs. Increased POD activity in the gill tissue of crayfish induced by WSSV was also observed by Wang et al. [36].

## 5. Conclusions

In conclusion, we established a qPCR-based method to quantify the number of *Mesanoophrys* sp. An obvious increase in *Mesanoophrys* sp. could be detected by the qPCR in all six of the tissues as early as 3 h post-infection, and the highest mortality of the infected *S. paramamosain* was found within the first 24 h following infection. The gill tissue was the main target of *Mesanoophrys* sp. Infection, with the high parasitic DNA loads causing obvious damage to the filament structure. Meanwhile, the activity of antioxidant enzymes in three representative tissues was significantly increased in the infected group at certain time points, indicating the immune defenses of *S. paramamosain* had been triggered by *Mesanoophrys* sp. infection. Our study provides useful information for further research on the mechanisms underpinning the pathogenesis of *Mesanoophrys* sp. in *S. paramamosain* and may also contribute to the further control of *Mesanoophrys* sp. However, these results were based on experimentally injected *S. paramamosain*, and further research will be needed to investigate the process and effect of *Mesanoophrys* sp. on naturally infected *S. paramamosain*, which might yield different results.

**Author Contributions:** Conceptualization, R.L. and C.W.; Methodology, K.Z. and R.L.; Formal analysis, K.Z. and W.Z.; Investigation, K.Z., W.Z., J.L., Q.C., H.H., F.Y., C.M. and W.S.; Writing—original draft preparation, K.Z., W.Z. and R.L.; Writing—review and editing, funding acquisition, R.L. and C.W. All authors have read and agreed to the published version of the manuscript.

**Funding:** This research and APC were funded by Key Scientific and Technological Grant of Zhejiang for Breeding New Agricultural Varieties (2021C02069-6), Ministry of Agriculture of China & China Agriculture Research System (no: CARS-48), 2025 Technological Innovation for Ningbo (2019B10010) and K.C. Wong Magana Fund in Ningbo University.

**Institutional Review Board Statement:** This study was approved by the Ethics Committee of Ningbo University (no. 20190410-042) and conducted according to relevant national and international guidelines.

**Informed Consent Statement:** Not applicable.

**Data Availability Statement:** The data supporting these findings of this study are included in the manuscript.

**Conflicts of Interest:** None of the authors has any conflict of interest to declare.

## References

1. Waiho, K.; Fazhan, H.; Quinitio, E.T.; Baylon, J.C.; Fujaya, Y.; Azmie, G.; Wu, Q.; Shi, X.; Ikhwanuddin, M.; Ma, H. Larval rearing of mud crab (*Scylla*): What lies ahead. *Aquaculture* **2018**, *493*, 37–50. [\[CrossRef\]](#)
2. Sathiadhas, R.; Najmudeen, T. Economic evaluation of mud crab farming under different production systems in India. *Aquac. Econ. Manag.* **2004**, *8*, 99–110. [\[CrossRef\]](#)
3. Fazhan, H.; Waiho, K.; Norfaizza, W.I.W.; Megat, F.H.; Ikhwantddin, M. Inter-species mating among mud crab genus *Scylla* in captivity. *Aquaculture* **2017**, *471*, 49–54. [\[CrossRef\]](#)
4. Syafaat, M.N.; Azra, M.N.; Waiho, K.; Fazhan, H.; Abol-Munafi, A.B.; Ishak, S.D.; Syahnon, M.; Ghazali, A.; Ma, H.; Ikhwanuddin, M. A Review of the Nursery Culture of Mud Crabs, Genus *Scylla*: Current Progress and Future Directions. *Animals* **2021**, *11*, 2034. [\[CrossRef\]](#) [\[PubMed\]](#)
5. Kong, T.; Ren, X.; Lin, S.; Li, S.; Gong, Y. Elucidation of metabolic responses in mud crab *Scylla paramamosain* challenged to WSSV infection by integration of metabolomics and transcriptomics. *Dev. Comp. Immunol.* **2020**, *113*, 103799. [\[CrossRef\]](#) [\[PubMed\]](#)
6. Wang, J.; Hong, W.J.; Zhu, F. The role of astakine in *Scylla paramamosain* against *Vibrio Alginolyticus* and white spot syndrome virus infection. *Fish Shellfish Immunol.* **2020**, *98*, 236–244. [\[CrossRef\]](#)
7. Song, W.B.; Zhu, M.Z.; Chen, Z.G.; Wang, M. Diagnostic assessment of some common pathogenic genera within the order *Scuticociliatida*: Members inhabiting mariculture biotopes. *J. Qingdao Ocean Univ.* **2000**, *30*, 207–216.
8. Yu, Y.; Kong, J.; Perveen, S.; Lei, Y.; Feng, B.; Yang, L.; Yin, F. Anti-parasitic effects of quinine sulfate on the swimming crab parasite *Mesanothryx* sp. *Aquaculture* **2021**, *544*, 737071. [\[CrossRef\]](#)
9. Perveen, S.; Lei, Y.H.; Yin, F.; Wang, C.L. Effect of environmental factors on survival and population growth of ciliated parasite, *Mesanothryx* sp. (Ciliophora: Scuticociliatida) infecting *Portunus trituberculatus*. *Parasitology* **2021**, *148*, 477–485. [\[CrossRef\]](#)
10. Lei, Y.H.; Perveen, S.; Xie, X.; Yang, L.J.; Gao, Q.X.; Wang, C.L.; Yin, F. Host-parasite interactions: A study on the pathogenicity of *Mesanothryx* sp. and hemocytes-mediated parasitic resistance of swimming crabs (*Portunus trituberculatus*) at different temperatures. *Aquaculture* **2022**, *551*, 737920. [\[CrossRef\]](#)
11. Liu, X.; Lei, Y.; Ren, Z.; Zhou, S.; Qian, D.; Yu, Y.; Yin, F.; Wang, C. Isolation, characterization and virulence of *Mesanothryx* sp. (Ciliophora: Orchitophryidae) in farmed swimming crab (*Portunus trituberculatus*) in eastern China. *Fish Dis.* **2020**, *43*, 1419–1429. [\[CrossRef\]](#) [\[PubMed\]](#)
12. Yu, Y.; Liu, X.; Lei, Y.; Zhou, S.; Jin, S.; Qian, D.; Xie, X.; Yin, F.; Wang, C. Anti-parasitic effects and toxicity of formalin on the parasite *Mesanothryx* sp. of the swimming crab *Portunus trituberculatus*. *Exp. Parasitol.* **2020**, *212*, 107886. [\[CrossRef\]](#) [\[PubMed\]](#)
13. Wang, J.F.; Li, M.; Xiao, J.; Xu, W.J.; Li, C.W. *Hematodinium* spp. infections in wild and cultured populations of marine crustaceans along the coast of China. *Dis. Aquat. Org.* **2017**, *124*, 181–191. [\[CrossRef\]](#) [\[PubMed\]](#)
14. Coates, C.J.; Rowley, A.F. Emerging diseases and epizootics in crabs under cultivation. *Front. Mar. Sci.* **2022**, *8*, e809759. [\[CrossRef\]](#)
15. Midorikawa, Y.; Shimizu, T.; Sanda, T.; Hamasaki, K.; Dan, S.; Lal, M.T.B.M.; Kato, G.; Sano, M. Characterization of *Aquimarina hainanensis* isolated from diseased mud crab *Scylla serrata* larvae in a hatchery. *J. Fish Dis.* **2020**, *43*, 541–549. [\[CrossRef\]](#)
16. Groben, G.; Clarke, B.B.; Murphy, J.A.; Koch, P.L.; Crouch, J.A.; Lee, S.; Zhang, N. Real-time PCR detection of *Clavosporium* spp., the causal agents of dollar spot in turfgrasses. *Plant Dis.* **2020**, *104*, 3118–3123. [\[CrossRef\]](#)
17. Wang, L.; Lv, Q.; He, Y.; Gu, R.; Zhou, B.; Chen, J.; Fan, X.; Pan, G.; Long, M.; Zhou, Z. Integrated qPCR and staining methods for detection and quantification of *Enterocytozoon hepatopenaei* in Shrimp *Litopenaeus vannamei*. *Microorganisms* **2020**, *8*, 1366. [\[CrossRef\]](#)
18. Cain, T.A.; Morado, J.F. Changes in total hemocyte and differential counts in Dungeness crabs infected with *Mesanothryx pugettensis*, a marine facultative parasitic ciliate. *Aquat. Anim. Health.* **2001**, *13*, 310–319. [\[CrossRef\]](#)
19. Parama, A.; Iglesias, R.; Alvarez, M.F.; Leiro, J.; Aja, C.; Sanmartin, M.L. *Philasterides dicentrarchi* (Ciliophora, Scuticociliatida): Experimental infection and possible routes of entry in farmed turbot (*Scophthalmus maximus*). *Aquaculture* **2003**, *217*, 73–80. [\[CrossRef\]](#)
20. Stentiford, G.D.; Shields, J.D. A review of the parasitic dinoflagellates *Hematodinium* species and *Hematodinium*-like infections in marine crustaceans. *Dis. Aquat. Org.* **2005**, *66*, 47–70. [\[CrossRef\]](#)
21. Perveen, S.; Yang, L.; Xie, X.; Han, X.; Gao, Q.; Wang, J.; Wang, C.; Yin, F. Vitamin C elicits the activation of immunological responses in swimming crab (*Portunus trituberculatus*) hemocytes against *Mesanothryx* sp. *Aquaculture* **2022**, *547*, 737447. [\[CrossRef\]](#)
22. Chen, W.F.; Fu, Y.W.; Zeng, Z.Y.; Guo, S.Q.; Yan, Y.L.; Tu, Y.F.; Guo, T.G.; Zhang, Q.Z. Establishment and application of a TaqMan probe-based qPCR for the detection of *Enterocytozoon hepatopenaei* in shrimp *Litopenaeus vannamei*. *Parasitol. Res.* **2022**, *121*, 2263–2274. [\[CrossRef\]](#) [\[PubMed\]](#)
23. Liu, Y.M.; Qiu, L.; Sheng, A.Z.; Wan, X.Y.; Cheng, D.Y.; Huang, J. Quantitative detection method of *Enterocytozoon hepatopenaei* using TaqMan probe real-time PCR. *J. Invertebr. Pathol.* **2018**, *151*, 191–196. [\[CrossRef\]](#) [\[PubMed\]](#)

24. Correya, M.S.; Vijayagopal, P.; Sanil, N.K. Morphological and molecular description of a new species of *Myxobolus* (*Myxosporea: Myxobolidae*) infecting *Planiliza macrolepis* (Smith, 1846) from India. *J. Parasit. Dis.* **2021**, *45*, 887–896. [[CrossRef](#)]
25. Frischer, M.E.; Landers, S.C.; Walker, A.N.; Powell, S.A.; Lee, R.F. Black gill in marine decapod crustaceans: A review. *Rev. Fish. Sci. Aquac.* **2022**, *30*, 498–519. [[CrossRef](#)]
26. Morado, J.F.; Small, E.B. Ciliate parasites and related diseases of crustacea: A review. *Fish Res.* **1995**, *3*, 275–354. [[CrossRef](#)]
27. Cheng, C.H.; Ma, H.L.; Liu, G.X.; Deng, Y.Q.; Jiang, J.J.; Feng, J.; Guo, Z.X. Biochemical, metabolic, and immune responses of mud crab (*Scylla paramamosain*) after mud crab reovirus infection. *Fish Shellfish Immunol.* **2022**, *127*, 437–445. [[CrossRef](#)]
28. Roma, E.H.; Macedo, J.P.; Goes, G.R.; Gonçalves, J.L.; Castro, W.D.; Cisalpino, D.; Vieira, L.Q. Impact of reactive oxygen species (ROS) on the control of parasite loads and inflammation in *Leishmania amazonensis* infection. *Parasit. Vectors* **2016**, *9*, 193. [[CrossRef](#)]
29. Tu, D.D.; Zhou, Y.L.; Gu, W.B.; Zhu, Q.H.; Xu, B.P.; Zhou, Z.K.; Liu, Z.P.; Wang, C.; Chen, Y.Y.; Shu, M.A. Identification and characterization of six peroxiredoxin transcripts from mud crab *Scylla paramamosain*: The first evidence of peroxiredoxin genefamily in the entire antioxidant defence grid. *Mol. Immunol.* **2018**, *93*, 223–235.
30. Cecerska-Heryc, E.; Surowska, O.; Heryc, R.; Serwin, N.; Napiontek-Balinska, S.; Dołęgowska, B. Are antioxidant enzymes essential markers in the diagnosis and monitoring of cancer patients—A review. *Clin. Biochem.* **2021**, *93*, 1–8. [[CrossRef](#)]
31. Zalewska-Ziob, M.; Adamek, B.; Kasperczyk, J.; Romuk, E.; Hudziec, E.; Chwalinska, E.; Dobija-Kubica, K.; Rogozinski, P.; Brulinski, K. Activity of antioxidant enzymes in the tumor and adjacent noncancerous tissues of non-small-cell lung cancer. *Oxid. Med. Cell Longev.* **2019**, *31*, 2901840. [[CrossRef](#)] [[PubMed](#)]
32. Mittle, R.; Vanderauwera, S.; Gollery, M.; Van Breusegem, F. Reactive oxygen gene network of plants. *Trends Plant. Sci.* **2004**, *9*, 490–498. [[CrossRef](#)] [[PubMed](#)]
33. Hong, Y.H.; Huang, Y.; Yan, G.W.; Pan, C.; Zhang, J.L. Antioxidative status, immunological responses, and heat shock protein expression in hepatopancreas of Chinese mitten crab, *Eriocheir sinensis* under the exposure of glyphosate. *Fish Shellfish Immunol.* **2019**, *86*, 840–845. [[CrossRef](#)]
34. Ighodaro, O.M.; Akinloye, O.A. First line defence antioxidants-superoxide dismutase (SOD), catalase (CAT) and glutathione peroxidase (GPX): Their fundamental role in the entire antioxidant defence grid. *Alex. J. Med.* **2018**, *54*, 287–293. [[CrossRef](#)]
35. Xu, J.X.; Cao, C.Y.; Sun, Y.C.; Wang, L.L.; Li, N.; Xu, S.W.; Li, J.L. Effects on liver hydrogen peroxide metabolism induced by dietary selenium deficiency or excess in chickens. *Biol. Trace Elem. Res.* **2014**, *159*, 174–182. [[CrossRef](#)]
36. Wang, D.L.; Zuo, D.; Wang, L.M.; Sun, T.; Wang, Q.; Zhao, Y.L. Effects of white spot syndrome virus infection on immuno-enzyme activities and ultrastructure in gills of *Cherax quadricarinatus*. *Fish Shellfish Immunol.* **2012**, *32*, 645–650. [[CrossRef](#)]

**Disclaimer/Publisher’s Note:** The statements, opinions and data contained in all publications are solely those of the individual author(s) and contributor(s) and not of MDPI and/or the editor(s). MDPI and/or the editor(s) disclaim responsibility for any injury to people or property resulting from any ideas, methods, instructions or products referred to in the content.